



HAL
open science

Evidence of high Sr/Ca in a Middle Jurassic murolith coccolith species

Baptiste Suchéras-Marx, Fabienne Giraud, Alexandre S. Simionovici, Rémi Tucoulou, Isabelle Daniel

► **To cite this version:**

Baptiste Suchéras-Marx, Fabienne Giraud, Alexandre S. Simionovici, Rémi Tucoulou, Isabelle Daniel. Evidence of high Sr/Ca in a Middle Jurassic murolith coccolith species. Peer Community In Paleontology, 2020, 10.31233/osf.io/dcfuq . hal-03167041

HAL Id: hal-03167041

<https://hal.science/hal-03167041>

Submitted on 11 Mar 2021

HAL is a multi-disciplinary open access archive for the deposit and dissemination of scientific research documents, whether they are published or not. The documents may come from teaching and research institutions in France or abroad, or from public or private research centers.

L'archive ouverte pluridisciplinaire **HAL**, est destinée au dépôt et à la diffusion de documents scientifiques de niveau recherche, publiés ou non, émanant des établissements d'enseignement et de recherche français ou étrangers, des laboratoires publics ou privés.




Distributed under a Creative Commons Attribution - NonCommercial - ShareAlike 4.0 International License



Evidence of high Sr/Ca in a Middle Jurassic muroolith coccolith species

RESEARCH ARTICLE

Baptiste Suchéras-Marx¹ , Fabienne Giraud^{2,3}, Alexandre Simionovici^{2,3,*}, Rémi Tucoulou⁴, & Isabelle Daniel⁵

Cite as: Suchéras-Marx B, Giraud F, Simionovici A, Tucoulou R, and Daniel I (2020). Evidence of high Sr/Ca in a Middle Jurassic muroolith coccolith species. *PaleorXiv*, dcfuq, version 7, peer-reviewed by PCI Paleo. DOI: 10.31233/osf.io/dcfuq

Published: 20 October 2020

Recommender:
Antonino Briguglio

Reviewers:
Kenneth De Baets and an anonymous reviewer

Correspondence:
sucheras-marx@cerege.fr



© 2020 Author(s)



This work is licensed under the Creative Commons Attribution 4.0 International License.

¹ Aix-Marseille Université, CNRS, IRD, Collège de France, CEREGE UM34 – Aix-en-Provence, France

² Université Grenoble-Alpes, ISTerre – Grenoble, France

³ CNRS, ISTerre – Grenoble, France

⁴ ESRF – The European Synchrotron Radiation Facility – Grenoble, France

⁵ UMR CNRS 5276 LGL, Université Claude Bernard Lyon 1, Ecole Normale Supérieure de Lyon – Villeurbanne, France

* Institut Universitaire de France (IUF)

THIS ARTICLE HAS BEEN PEER-REVIEWED BY PCI PALEO

Read the Editor's recommendation and Referees' reports at [DOI:10.24072/pci.paleo.100006](https://doi.org/10.24072/pci.paleo.100006)

Abstract

Paleoceanographical reconstructions are often based on microfossil geochemical analyses. Coccoliths are the most ancient, abundant and continuous record of pelagic photic zone calcite producer organisms. Hence, they could be valuable substrates for geochemically based paleoenvironmental reconstructions but only Sr/Ca is exploited even if it remains poorly understood. For example, some muroolith coccoliths species have very high Sr/Ca compared to the common 1-4 mmol/mol recorded in placolith coccoliths. In this study, we analyzed the elemental composition of the Middle Jurassic muroolith *Crepidolithus crassus* by synchrotron-based nanoXRF (X-ray Fluorescence Spectroscopy) mapping focusing on Sr/Ca and compared the record to two placolith species, namely *Watznaueria contracta* and *Discorhabdus striatus*. In *C. crassus*, Sr/Ca is more than ten times higher than in both placoliths and seems higher in the proximal cycle. By comparison with the placoliths analyzed in the same analytical set-up and from the same sample, we exclude the impact of the diagenesis and seawater Sr/Ca to explain the high Sr/Ca in *C. crassus*. Based on comparisons to *Pontosphaera discopora* and *Scyphosphaera apsteinii* which also have high Sr/Ca, it seems more likely that high Sr/Ca in *C. crassus* is either due to the vertical elongation of the R-units of the proximal cycle or related to the action of the special polysaccharide controlling the growth of those vertically elongated R-units that may have affinities to Sr²⁺. In order to apply the Sr/Ca proxy to murooliths, further investigations are needed on cultured coccoliths.

Keywords: Calcareous nannofossils; Coccoliths; ESRF; Murooliths; Sr/Ca; Ultrastructure; XRF

Introduction

Paleoceanography partly relies on the application of geochemical proxies – i.e. chemical changes of fossils or sediments composition induced by chemical, physical or biological parameters changing through time. Many geochemical proxies are based on elemental ratios in planktic or benthic foraminifera e.g. Mg/Ca (temperature; [Elderfield and Ganssen, 2000](#)), B/Ca (pH, [Yu et al., 2007](#)), U/Ca (carbonate saturation, [Raitzsch et al., 2011](#)), Cd/Ca (paleonutrient, [Rickaby and Elderfield, 1999](#)). Conversely, calcareous nanofossils – the micrometric platelets called coccoliths produced by the photosynthetic unicellular algae called coccolithophores and other micrometric calcite invertebrate shells – are rarely used for geochemistry in paleoceanography. The rarity of nanofossil-based geochemical paleoproxies is linked to the very small size of calcareous nanofossils – i.e. $\sim 1\text{--}15\ \mu\text{m}$ – increasing the difficulty to isolate them from the rest of the sediment ([Stoll and Ziveri, 2002](#); [Minoletti et al., 2009](#); [Stoll and Shimizu, 2009](#); [Suchéras-Marx et al., 2016b](#)). The only proxy commonly based on the calcareous nanofossil chemical composition is the Sr/Ca ratio used as a paleoproductivity proxy ([Stoll and Schrag, 2000](#)).

The most important factors influencing Sr/Ca ratios in biogenic carbonates is outlined in [Ullmann et al. \(2013\)](#) and are: i) the composition of the liquid from which they are precipitated ($\sim 8\ \text{mmol/mol}$ for modern oceans according to [Lebrato et al., 2020](#); $\sim 5\ \text{mmol/mol}$ for the Middle Jurassic according to [Ullmann et al., 2013](#)); ii) the calcium carbonate polymorph; iii) the species specific fractionation of the Sr/Ca ratio; iv) metabolic controls on this fractionation factor; and v) water temperature. The Sr/Ca ratio in calcareous nanofossils is a relative proxy which has no quantitative calibration. The process underlying the positive relation between Sr/Ca and productivity stands on the observation that more Sr is incorporated in calcite with high calcification rates which positively correlates with high cell physiological rates. This proxy is also species-dependent or, at least, group-dependent ([Stoll and Ziveri, 2004](#)). The latter is discussed, the species-dependency may be related to different calcification physiologies ([Payne et al., 2008](#); [Suchéras-Marx et al., 2016a](#)) or to different partitioning coefficients in relation to different ultrastructure organizations and more precisely between V- and R- crystals in coccoliths ([Young et al., 1992](#)) theoretically possible ([Paquette and Reeder, 1995](#)) but still not observed ([Stoll and Ziveri, 2004](#)).

Recently, analyses on the cultured murolith *Scyphosphaera apsteinii* showed Sr/Ca $\sim 22\ \text{mmol/mol}$, an order of magnitude higher than the common $\sim 1\text{--}4\ \text{mmol/mol}$ measured in placoliths such as *Gephyrocapsa oceanica*, *Gephyrocapsa huxleyi*, *Calcidiscus leptoporus*, *Coccolithus pelagicus* or *Helicosphaera carteri* ([Stoll et al., 2007](#); [Hermoso et al., 2017](#)). [Hermoso et al. \(2017\)](#) also highlight observations of high Sr/Ca in fossil muroliths *Pontosphaera* (Pliocene) and *Crepidolithus* (Lower Jurassic) but points out that *Scyphosphaera*, *Pontosphaera* and *Crepidolithus* have different crystal organizations and growth directions and thus crystal organization cannot explain murolith high Sr/Ca.

The present study aims to map Sr and Ca in *Crepidolithus crassus* and to compare the calculated Sr/Ca with the crystal growth directions in order to explain the murolith Sr anomaly. This study will discuss then the range of applicability and limitation of the Sr/Ca proxy in coccoliths.

Material and methods

Material

The coccolith analyzed in this study comes from sample CM35, a marlstone from the lower Bajocian (Middle Jurassic) of Cabo Mondego (Portugal; section in [Suchéras-Marx et al., 2012](#)). This section was selected because it is the Aalenian-Bajocian boundary GSSP ([Pavia and Enay, 1997](#)). A total of three coccoliths from three different species were studied, namely the murolith *Crepidolithus crassus* and two placoliths *Discorhabdus striatus* and *Watznaueria contracta*.

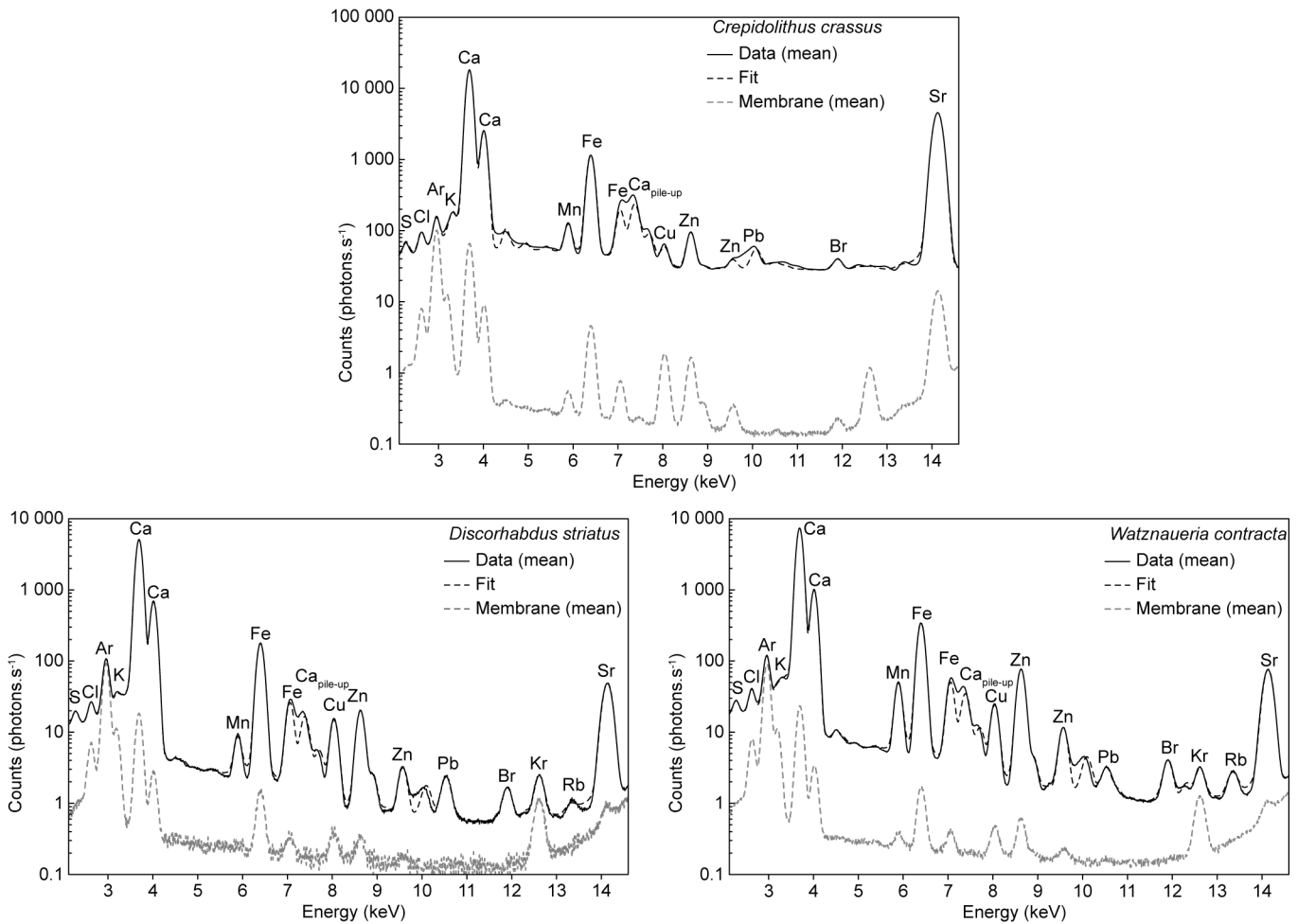


Figure 1. Mean XRF spectra of *C. crassus*, *D. striatus* and *W. contracta* coccoliths and associated membrane spectra. $Ca_{pile-up}$ corresponds to the quantification of two Ca energy summed arriving at the same time in the captor. Ar is the same in coccolith and membrane because it corresponds to the air in the experimental hutch. In the three coccoliths, membrane contribution in Ca, Fe, Cu and Zn and in Sr in *C. crassus* is observed. However, it is always two order of magnitude below the concentration in the coccolith thus membrane contribution represents less than 1% in those elements.

Sample preparation

The three coccoliths were picked using [Suchéras-Marx et al. \(2016b\)](#) protocol which consists in a hand-picking procedure. Rock powder is smeared on a cover slide in order to isolate particles from each other. Coccoliths are then observed with an optical microscope Leica DM750P with a x200 magnification (x20 dry objective) under cross-polarized light. Coccoliths are identified with a x400 magnification (x40 dry objective) and a $\lambda/4$ gypsum filter may be used if further optical criteria of recognition are needed. Once picked, each coccolith is mounted on 500 nm-thick silicon nitride (Si_3N_4) TEM windows (Silson Ltd. Southam, UK) using a drop of ethanol to detach the coccolith from the needle. No other chemical or physical treatment were made.

NanoXRF 17 keV mapping at ID22NI

The XRF analyses were performed at beamline ID22NI (currently ID16b) at the European Synchrotron Radiation Facility (ESRF), Grenoble, France. All three coccoliths were analyzed at an incident X-ray beam energy of 17 keV to ensure the measure of Sr ($K\alpha = 14.165$ keV). The beam spot was focused by an ESRF custom-made Kirkpatrick-Baez double multilayer mirror device to a 100 nm x 100 nm size. Each spot was

Table 1. Mn/Ca and Sr/Ca ratios. Mn/Ca and Sr/Ca (mmol/mol) of whole coccoliths of *C. crassus*, *D. striatus* and *W. contracta* or a selected region (see [Supplementary Figure S2](#)), depleted in Mn and Fe.

Element ratio (mmol/mol)	Mean whole coccolith		Selected zone	
	Mn/Ca	Sr/Ca	Mn/Ca	Sr/Ca
<i>Crepidolithus crassus</i>	0.75	9.82	0.92	17.70
<i>Discorhabdus striatus</i>	0.23	0.38	0.09	0.31
<i>Watznaueria contracta</i>	1.10	0.40	0.58	0.45

analyzed for 2 s. The detectors were high-count rate twin SII™vortex SDD (silicon drift diode) detectors, capable of counting up to 200 kcps with no saturation and no peak shift or FWHM broadening, when operated below 10% dead time. The sample is orthogonal to the incident beam and the detector is placed at a 15° angle relative to the sample surface. The three coccoliths were mapped. Each pixel corresponds to a spot of analysis and spots are adjacent providing a full map of each coccolith. *Crepidolithus crassus* map is 136 x 120 pixels large, *D. striatus* is 60 x 34 pixels large and *W. contracta* map is 100 x 74 pixels large. The XRF analysis being penetrative, the element counting sum up the membrane, the coccolith and the air surrounding the coccolith. The contribution of the air is negligible, and the contribution of the membranes are estimated in [Figure 1](#) based on quantification in zones without the coccolith in the maps. All calculations were made using PyMCA 5.1.1. ([Solé et al., 2007](#)). This beam line set-up, analysis procedure and calculation fit are the same as in [Suchéras-Marx et al. \(2016a\)](#).

Results

XRF spectrum

The three spectra shown in [Figure 1](#) represent the mean spectrum for each coccolith. Because XRF analysis is penetrative, the spectra also record the membrane holding the coccolith and thus the spectrum of zones with only the membrane is also presented. The fit presented for each spectrum is the modeled reconstruction used for the calculation and the map reconstruction (cps and mmol/mol). In *D. striatus* and *W. contracta*, 14 elements are recorded namely: S, Cl, Ar, K, Ca, Mn, Fe, Cu, Zn, Br, Kr, Rb, Sr and Pb whereas in *C. crassus* only 12 are recorded (same elements except Kr and Rb) ([Fig. 1](#)). The rare gases Ar and Kr are present in the air in the experimental hutch. The contribution of the membrane is lower than 1% for Ca and Sr and thus is negligible for the Sr/Ca calculation. Nevertheless, membrane contribution was excluded in [Table 1](#). Those results are similar to already published for *W. britannica* and *D. striatus* ([Suchéras-Marx et al., 2016a, 2020](#)).

Element and ratio maps

For the three coccoliths, element maps of Ca, Mn and Sr are presented in [Figure 2](#) (cps) and the three maps together in color in [Supplementary Figure S1](#). Direct comparison of Ca and Sr is possible in both placoliths whereas Mn is quite different although crystal organization is also observed in this element map. In *W. contracta*, the Ca maps are precise enough to recognize the shield crystal orientations, especially the outer radial growth from the tube ring. The tube structures are difficult to recognize but still, crystals can be seen in the rim around the central area. In the Sr map of the same species, the outer rim with radial crystals of the shields are easily observed too. A ring with slightly more Sr marks a boundary between the outer rim and the inner rim structures. These inner rim structures are composed of two concentric rings of crystal assemblages. The outermost one may correspond to the mid tube elements

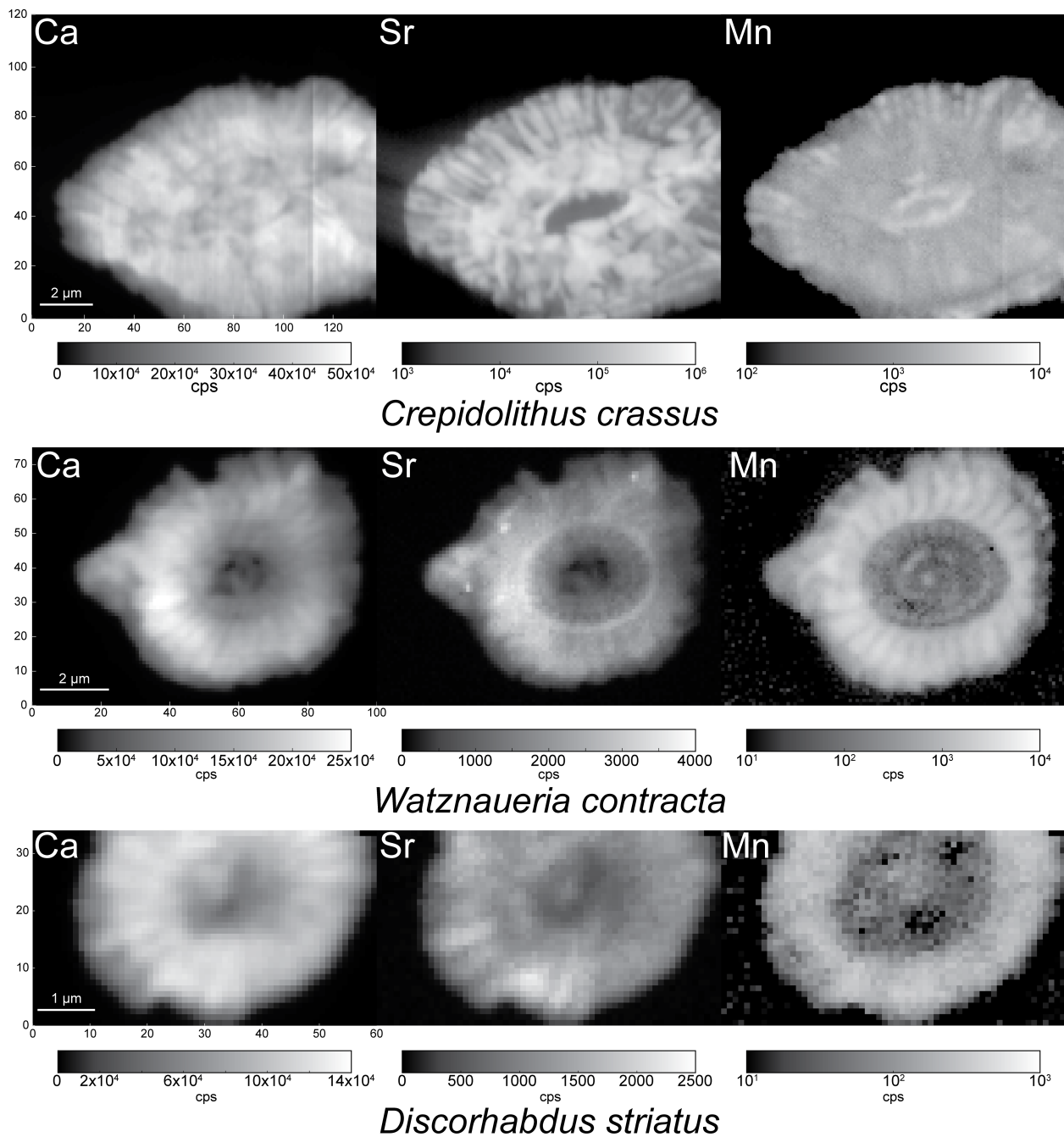


Figure 2. Ca, Sr and Mn maps (cps) of *C. crassus*, *D. striatus* and *W. contracta*.

whereas the innermost one may correspond to the inner tube elements. The mid tube elements form a clear rim whereas one shield crystal assemblage is nicely depicted in the Mn map (Suchéras-Marx et al., 2016a). In *D. striatus*, the Sr seems less abundant in the tube units in comparison to the shield elements. For the same species, the Mn is scarce in the central area and the tube structures but more abundant in the shields.

Conversely to the placoliths, in *C. crassus*, the Ca and Sr maps are slightly different. In Sr maps, the central area is easily visible. Around the central area, an inner concentric rim of more abundant Sr is observed. A concentric outer rim up to the lateral border is observed with Sr concentrated in radial rays. In the Ca map, the outer rim is also observed in radial structures but the inner rim is distinguished from

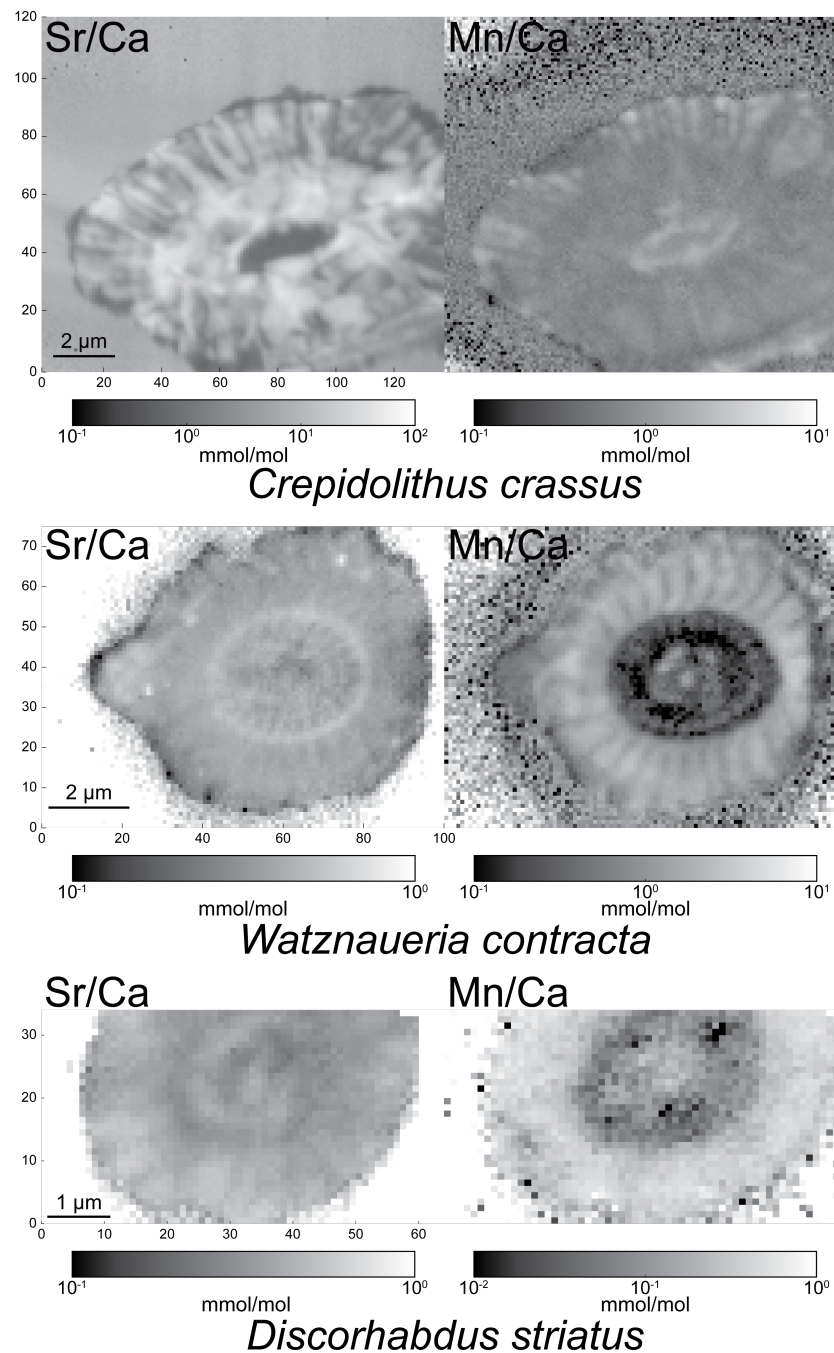


Figure 3. Sr/Ca and Mn/Ca maps (mmol/mol) of *C. crassus*, *D. striatus* and *W. contracta*.

the outer only by a discontinuity. Finally, another discontinuity separates the central area from the inner rim.

For all species, the Sr/Ca maps have the same patterns as Sr and similarly, the Mn/Ca maps have the same patterns as Mn (Fig. 3). In *C. crassus* then, the Sr/Ca is higher in a ring around the central area and in radially oriented crystals in the outer ring. In the most concentrated area, the Sr/Ca ranges between 10 and 100 mmol/mol and tends to be two orders of magnitude higher than in *W. contracta* and *D. striatus*. Finally, the area with higher Sr/Ca is neither enriched nor depleted in Mn/Ca.

Discussion

A previous study already discussed the Sr/Ca signal in *Watznaueria* (Suchéras-Marx et al., 2016a), discussion that likely applies to *Discorhabdus*. The presence of other elements such as Cl, Fe or Zn will not be discussed here to focus on Sr/Ca. Nevertheless, according to Suchéras-Marx et al. (2016a) Cl and S may be incorporated in the coccolith during coccolithogenesis whereas K, Fe, Cu, Zn, Br and Rb are incorporated during diagenesis or are contaminant from clays. Recently, Bottini et al. (2020) studied coccolith from controlled cultures confirmed that V, Fe, Ni, Zn and Pb are not incorporated in coccolith calcite; they also proposed that Cl is a contaminant from seawater not present in the coccolith crystal composition. Finally, the presence of Mn is related to overgrowth and diagenesis in both *Watznaueria* and *Discorhabdus* (Suchéras-Marx et al., 2016a, 2020). The three coccoliths are coming from the same sample and were analyzed with the same set-up, thus the very high Sr/Ca in *C. crassus* compared to *W. contracta* and *D. striatus* is not related to analytical biases and to seawater Sr/Ca. Moreover, the Sr-rich rim in *C. crassus* is not enriched in Mn and thus the high Sr/Ca in *C. crassus* is not related to diagenesis. Finally, the calculated Sr/Ca for the lower Bajocian seawater ranges between 4 mmol/mol and 6.8 mmol/mol (Ullmann et al., 2013) below most modern oceanic environments (Lebrato et al., 2020) and thus cannot explain the high Sr/Ca in *C. crassus*. This result is coherent with a previous study observing that diagenesis tends to lower Sr/Ca in calcareous nannofossils (Dedert et al., 2014) as Sr concentrations are relatively high in seawater and are low in diagenetic fluids (Veizer, 1974; James and Jones, 2015).

The Sr anomaly in *C. crassus* is then related to either: i) an ion pump concentrating the Sr²⁺ inside the cell to higher concentrations than other species; ii) the use of a polysaccharide that tends to increase Sr/Ca in comparison to other species; or iii) the crystal organization and growth directions which are controlled by the cell but the high concentration in Sr would then be a by-product of the coccolith construction. Obviously, *C. crassus* being a fossil occurring only during the Jurassic, the cell biology of the species cannot be explored. Nevertheless, this species is a large murolith like the extant *Pontosphaera discopora* and has a similar shape to the extant *Scyphosphaera apsteinii*'s lopadolith, both having also higher Sr/Ca than the common placolith signature of 1-4 mmol/mol (Hermoso et al., 2017).

The first two hypotheses (i.e. Sr²⁺ ion pump or special polysaccharide) could be that high Sr/Ca is inherited in descendant species from *C. crassus*. Both *Pontosphaera* and *Scyphosphaera* are very closely related in the coccolithophore phylogeny (family Pontosphaeraceae; De Vargas et al., 2007). *Crepidolithus* is within the family Chiastozygaceae, whose position is unknown, but could be the ancestor of the family Zygodiscaceae and its descendants, the families Pontosphaeraceae and Helicosphaeraceae (Bown and Young, 1998). Thus, the high Sr/Ca in both *Pontosphaera* and *Scyphosphaera* could be an ancestral character inherited from *Crepidolithus*. This hypothesis may be challenged by *Helicosphaera carterii* which has a Sr/Ca ratio around 2-3 mmol/mol (Stoll and Ziveri, 2004) and is from the family Helicosphaeraceae, the sister group of the family Pontosphaeraceae (Bown and Young, 1998). The low Sr/Ca in *H. carterii* could then be a derived character in the phylogeny, arguing for a phyletic heritage of *Pontosphaera* and *Scyphosphaera* from *Crepidolithus* or this character is ancestral in the family Helicosphaeraceae and the Sr/Ca is not linked to the phylogeny. The current knowledge on coccolithophore phylogeny and Sr/Ca cannot exclude one or the other solutions, hence a possible ion pump or polysaccharide could have favored the high Sr/Ca in *C. crassus*. Recently, Meyer et al. (2020) observed that Sr²⁺ and Ca²⁺ fluxes in the coccolith vesicle for coccolithogenesis does not solely govern Sr incorporation in the coccolith speculating that possible species-specific polysaccharides dedicated to a peculiar coccolith morphology may act in the high Sr/Ca observed in *Scyphosphaera*.

The last hypothesis relies on the fact that *C. crassus*, *P. discopora* and *S. apsteinii* have the same shape (i.e. murolith and lopadolith) and are very large coccoliths, thus the shape and size may influence the Sr incorporation in coccolith calcite. The large size of those coccoliths cannot be the main reason of high

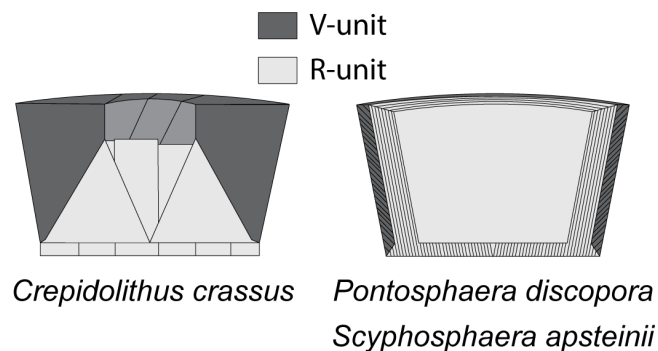


Figure 4. Crystal assembly of *Crepidolithus*, *Pontosphaera* and *Scyphosphaera*. R-units (light grey) and V-units (dark grey), derived from [Bown and Young \(1998\)](#).

Sr/Ca because *Coccolithus braarudii*, a very large placolith, has Sr/Ca equivalent to very small placoliths (i.e. *G. huxleyi*; [Müller et al., 2011](#)). The basic crystal organization of heterococcoliths is explained by the V/R model which describes the crystal growth in the c-axis whether radially (i.e. R- unit) or vertically (i.e. V-unit) from a primary ring of crystals called protococcolith ([Young et al., 1992](#)). In *C. crassus*, the V-units are more developed than the R-units ([Fig. 4](#)), whereas in *P. discopora* and *S. apsteinii* V-units represent only the narrow outer part of the rim wall ([Young and Bown, 1997](#); [Fig. 4](#)). According to [Hermoso et al. \(2017\)](#), the growth of calcite in the same direction as the c-axis should favor Sr²⁺ incorporation but the R-units in *P. discopora* and *S. apsteinii* actually grow longer in the vertical axis hence grow orthogonally to the c-axis. In the case of *C. crassus*, the Sr/Ca is higher around the central area which corresponds to the proximal cycle formed by R-units. Counterintuitively for these three species with thick vertical walls, the Sr is concentrated in the R-units. Surprisingly, *C. crassus* R-units are, like *P. discopora* and *S. apsteinii*, more elongated vertically than radially, thus the growth seems orthogonal to the c-axis ([Fig. 4](#)). Then, either the orthogonal to c-axis growth actually favors Sr²⁺ contradicting [Hermoso et al. \(2017\)](#) or the biomolecule acting in this growth direction has more affinities with Sr²⁺ than the other polysaccharides.

Conclusion

Despite the very high and continuous fossil record of coccoliths since the Late Triassic, the use of geochemical analyses on these calcite platelets for paleoenvironmental reconstructions remain rare. So far, coccolith Sr/Ca is the only coccolith-based geochemical proxy commonly used in paleoceanography. Yet, there are many unknown features about this productivity proxy such as the very high Sr/Ca (i.e. above ~10 mmol/mol) in some species namely *S. apsteinii*, *P. discopora* and *C. crassus*. In this study, we compared Sr/Ca of *C. crassus* to contemporaneous placoliths using synchrotron-based nanoXRF and observed that:

- *C. crassus* has higher Sr/Ca than contemporaneous placoliths;
- *C. crassus* Sr/Ca map is different than the Mn/Ca map;
- Sr/Ca in *C. crassus* is higher in the proximal cycle than in the distal cycle.

Hence, high *C. crassus* Sr/Ca, is not linked to diagenetic overgrowth or seawater Sr/Ca but may be related to vertical elongation of R-units and/or affinity to Sr²⁺ of the polysaccharide responsible for the growth of those peculiar R-units. The use of murolith's Sr/Ca in the future may be interesting due to their high values, easier to measure and to the large size of these coccoliths, easier to separate from the bulk placoliths. Nevertheless, in order to apply the Sr/Ca productivity proxy to muroliths in the future,

new culture studies should test the relation between Sr incorporation and growth rate. The study of *Pontosphaera* or *Scyphosphaera* with 3D nanoXRF will directly link Sr/Ca relative concentration with coccolith crystal organization and thus would clearly improve the understanding of the Sr anomaly in those coccoliths.

Acknowledgements

We acknowledge the ESRF for providing access to synchrotron radiation on the ID22NI beamline through proposal EC811. We deeply thank the recommender Antonino Briguglio and the reviewer Kenneth De Baets as well as the anonymous reviewer for suggestions that clearly improved the manuscript. BSM is particularly proud to be recommended by PCI Paleo and hope this editorial model will develop in the future. This study is a contribution to the Cerege's team 'Climat'.

Additional information

Funding

No funding information.

Competing interests

The authors declare they have no personal or financial conflict of interest relating to the content of this study.

Author contributions

BSM, FG and ID designed the study with later contribution from AS. BSM, FG, ID, AS and RT did the analyses. BSM performed the data treatment with help from AS. BSM wrote the manuscript with comments from all contributors.

Data availability

Data presented in this study are freely accessible on the PANGAEA database:

- DOI: 10.1594/PANGAEA.913826

Related data produced with similar material and during the same ESRF experiment (project EC811) are also accessible on PANGAEA:

- DOI: 10.1594/PANGAEA.913813 from [Suchéras-Marx et al. \(2016a\)](#)
- DOI: 10.1594/PANGAEA.913811 from [Suchéras-Marx et al. \(2020\)](#)
- DOI: 10.1594/PANGAEA.914203 (unpublished data)

Supplementary information

- Analyzed data are openly available on PANGAEA (see above)
- [Supplementary Figures S1–S2](#) appear at the end of this PDF

References

- Bottini C, Dapiaggi M, Erba E, Faucher G, and Rotiroti N (2020). High resolution spatial analyses of trace elements in coccoliths reveal new insights into element incorporation in coccolithophore calcite. *Scientific Reports* 10, 9825. doi: 10.1038/s41598-020-66503-x.
- Bown PR and Young JR (1998). Introduction. In: *Calcareous Nannofossil Biostratigraphy*. Ed. by Bown PR. British Micropalaeontological Society Publication Series. Dordrecht: Chapman and Hall (Kluwer Academic Publishers), pp. 1–15. isbn: 978-94-010-6056-1.
- De Vargas C, Aubry MP, Probert I, and Young J (2007). Origin and evolution of coccolithophores: from coastal hunters to oceanic farmers. In: *Evolution of Primary Producers in the Sea*. Ed. by Falkowski PG and Knoll A. San Diego: Academic Press, pp. 251–285. isbn: 978-0-12-370518-1.
- Dedert M, Stoll H, Kars S, Young JR, Shimizu N, Kroon D, Lourens L, and Ziveri P (2014). Temporally variable diagenetic overgrowth on deep-sea nannofossil carbonates across Palaeogene hyperthermals and implications for isotopic analyses. *Marine Micropaleontology* 107, 18–31. doi: 10.1016/j.marmicro.2013.12.004.
- Elderfield H and Ganssen G (2000). Past temperature and $\delta^{18}\text{O}$ of surface ocean waters inferred from foraminiferal Mg/Ca ratios. *Nature* 405, 442–445. doi: 10.1038/35013033.
- Hermoso M, Lefevre B, Minoletti F, and Raféls M de (2017). Extreme strontium concentrations reveal specific biomineralization pathways in certain coccolithophores with implications for the Sr/Ca paleoproductivity proxy. *PLOS ONE* 12, e0185655. doi: 10.1371/journal.pone.0185655.
- James NP and Jones B (2015). *Origin of carbonate sedimentary rocks*. Chichester: Wiley & Sons, Ltd. isbn: 978-1-118-65267-1.
- Lebrato M, Garbe-Schönberg D, Müller MN, Blanco-Ameijeiras S, Feely RA, Lorenzoni L, Molinero JC, Bremer K, Jones DOB, Iglesias-Rodríguez D, Greeley D, Lamare MD, Paulmier A, Graco M, Cartes J, Barcelos e Ramos J, Lara A de, Sanchez-Leal R, Jimenez P, Paparazzo FE, Hartman SE, Westernströer U, Küter M, Benavides R, Silva AF da, Bell S, Payne C, Olafsdottir S, Robinson K, Jantunen LM, Korablev A, Webster RJ, Jones EM, Gilg O, Bailly du Bois P, Beldowski J, Ashjian C, Yahia ND, Twining B, Chen XG, Tseng LC, Hwang JS, Dahms HU, and Oschlies A (2020). Global variability in seawater Mg:Ca and Sr:Ca ratios in the modern ocean. *Proceedings of the National Academy of Sciences* 117, 22281–22292. doi: 10.1073/pnas.1918943117.
- Meyer EM, Langer G, Brownlee C, Wheeler GL, and Taylor AR (2020). Sr in coccoliths of *Scyphosphaera apsteinii*: Partitioning behavior and role in coccolith morphogenesis. *Geochimica et Cosmochimica Acta* 285, 41–54. doi: 10.1016/j.gca.2020.06.023.
- Minoletti F, Hermoso M, and Gressier V (2009). Separation of sedimentary micron-sized particles for palaeoceanography and calcareous nannoplankton biogeochemistry. *Nature Protocols* 4, 14–24. doi: 10.1038/nprot.2008.200.
- Müller MN, Kısakürek B, Buhl D, Gutperlet R, Kolevica A, Riebesell U, Stoll H, and Eisenhauer A (2011). Response of the coccolithophores *Emiliania huxleyi* and *Coccolithus braarudii* to changing seawater Mg^{2+} and Ca^{2+} concentrations: Mg/Ca, Sr/Ca ratios and $\delta^{44/40}\text{Ca}$, $\delta^{26/24}\text{Mg}$ of coccolith calcite. *Geochimica et Cosmochimica Acta* 75, 2088–2102. doi: 10.1016/j.gca.2011.01.035.
- Paquette J and Reeder RJ (1995). Relationship between surface structure, growth mechanism, and trace element incorporation in calcite. *Geochimica et Cosmochimica Acta* 59, 735–749. doi: 10.1016/0016-7037(95)00004-J.
- Pavia G and Enay R (1997). Definition of the Aalenian-Bajocian Stage boundary. *Episodes* 20, 16–22.
- Payne VE, Rickaby REM, Benning LG, and Shaw S (2008). Calcite crystal growth orientation: implications for trace metal uptake into coccoliths. *Mineralogical Magazine* 72, 269–272. doi: 10.1180/minmag.2008.072.1.269.

- Raitzsch M, Kuhnert H, Hathorne EC, Groeneveld J, and Bickert T (2011). U/Ca in benthic foraminifers: A proxy for the deep-sea carbonate saturation. *Geochemistry, Geophysics, Geosystems* 12, Q06019. doi: 10.1029/2010GC003344.
- Rickaby REM and Elderfield H (1999). Planktonic foraminiferal Cd/Ca: Paleonutrients or paleotemperature? *Paleoceanography* 14, 293–303. doi: 10.1029/1999PA900007.
- Solé VA, Papillon E, Cotte M, Walter P, and Susini J (2007). A multiplatform code for the analysis of energy-dispersive X-ray fluorescence spectra. *Spectrochimica Acta Part B: Atomic Spectroscopy* 62, 63–68. doi: 10.1016/j.sab.2006.12.002.
- Stoll H, Shimizu N, Arevalos A, Matell N, Banasiak A, and Zeren S (2007). Insights on coccolith chemistry from a new ion probe method for analysis of individually picked coccoliths. *Geochemistry, Geophysics, Geosystems* 8, Q06020. doi: 10.1029/2006GC001546.
- Stoll HM and Schrag DP (2000). Coccolith Sr/Ca as a new indicator of coccolithophorid calcification and growth rate. *Geochemistry, Geophysics, Geosystems* 1, 1006. doi: 10.1029/1999GC000015.
- Stoll HM and Shimizu N (2009). Micropicking of nanofossils in preparation for analysis by secondary ion mass spectrometry. *Nature Protocols* 4, 1038–1043. doi: 10.1038/nprot.2009.83.
- Stoll HM and Ziveri P (2002). Separation of monospecific and restricted coccolith assemblages from sediments using differential settling velocity. *Marine Micropaleontology* 46, 209–221. doi: 10.1016/S0377-8398(02)00040-3.
- Stoll HM and Ziveri P (2004). Coccolithophorid-based geochemical paleoproxies. In: *Coccolithophores: From molecular processes to global impact*. Ed. by Thierstein HR and Young JR. Berlin, Heidelberg: Springer, pp. 529–562. isbn: 978-3-642-06016-8.
- Suchéras-Marx B, Giraud F, Simionovici A, Daniel I, and Tucoulou R (2016a). Perspectives on heterococcolith geochemical proxies based on high-resolution X-ray fluorescence mapping. *Geobiology* 14, 390–403. doi: 10.1111/gbi.12177.
- Suchéras-Marx B, Giraud F, Daniel I, Rivard C, Aubry MP, Baumann KH, Beaufort L, Tucoulou R, and Simionovici A (2020). Origin of manganese in nanofossil calcite based on synchrotron nanoXRF and XANES. *PaleorXiv*, p8cn5. doi: 10.31233/osf.io/p8cn5.
- Suchéras-Marx B, Giraud F, Lena A, and Simionovici A (2016b). Picking nanofossils: How and why. *Journal of Micropalaeontology* 36, 219–221. doi: 10.1144/jmpaleo2016-013.
- Suchéras-Marx B, Guihou A, Giraud F, Lécuyer C, Allemand P, Pittet B, and Mattioli E (2012). Impact of the Middle Jurassic diversification of *Watznaueria* (coccolith-bearing algae) on the carbon cycle and $\delta^{13}\text{C}$ of bulk marine carbonates. *Global and Planetary Change* 86–87, 92–100. doi: 10.1016/j.gloplacha.2012.02.007.
- Ullmann CV, Hesselbo SP, and Korte C (2013). Tectonic forcing of Early to Middle Jurassic seawater Sr/Ca. *Geology* 41, 1211–1214. doi: 10.1130/G34817.1.
- Veizer J (1974). Chemical diagenesis of belemnite shells and possible consequences for paleotemperature determinations. *Neues Jahrbuch für Geologie und Paläontologie, Abhandlungen* 147, 91–111.
- Young JR and Bown PR (1997). Higher classification of calcareous nanofossils. *Journal of Nannoplankton Research* 19, 15–20.
- Young JR, Didymus JM, Brown PR, Prins B, and Mann S (1992). Crystal assembly and phylogenetic evolution in heterococcoliths. *Nature* 356, 516–518. doi: 10.1038/356516a0.
- Yu J, Elderfield H, and Hönisch B (2007). B/Ca in planktonic foraminifera as a proxy for surface seawater pH. *Paleoceanography* 22, PA2202. doi: 10.1029/2006PA001347.

Ca (blue) – Sr (red) – Mn (green) (free scale cps)

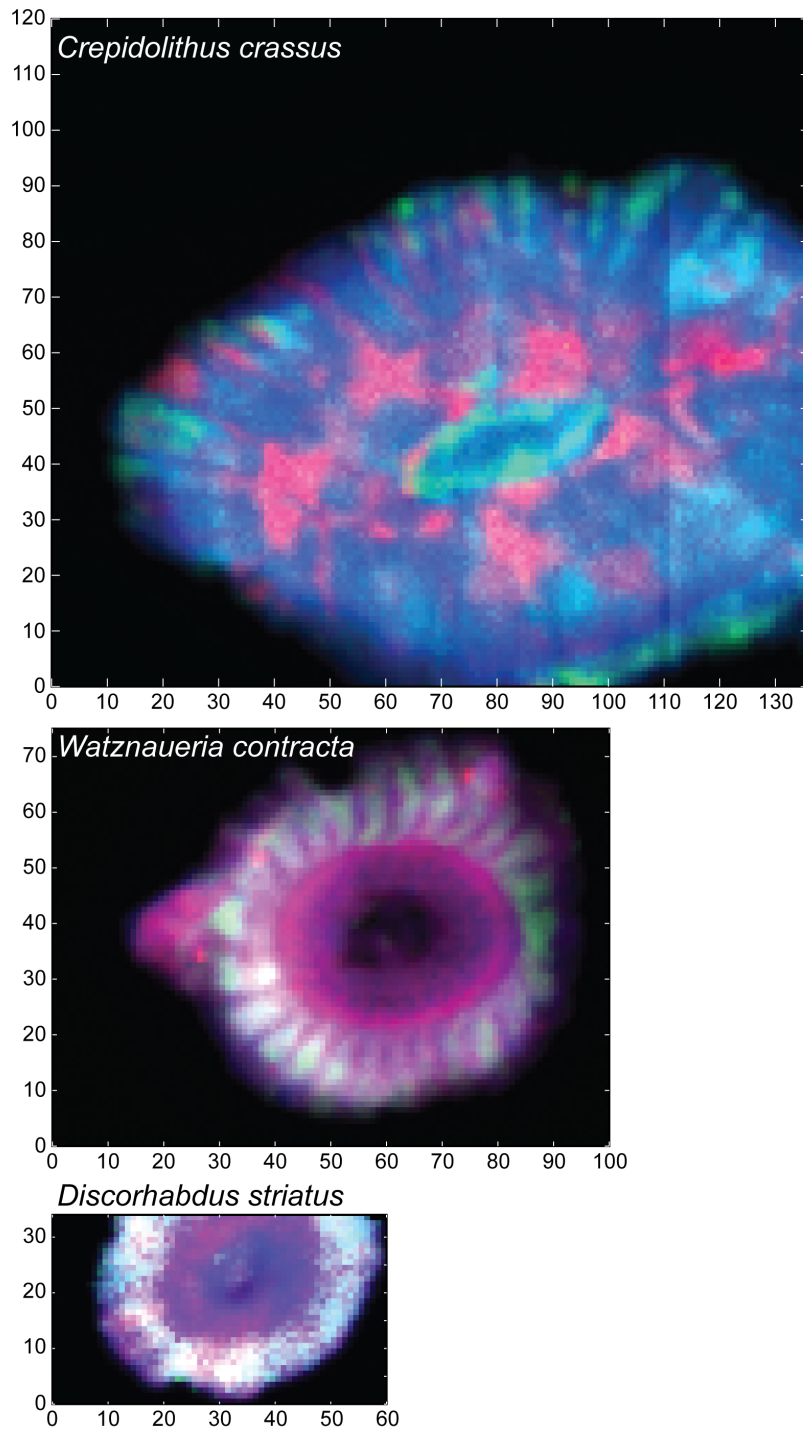
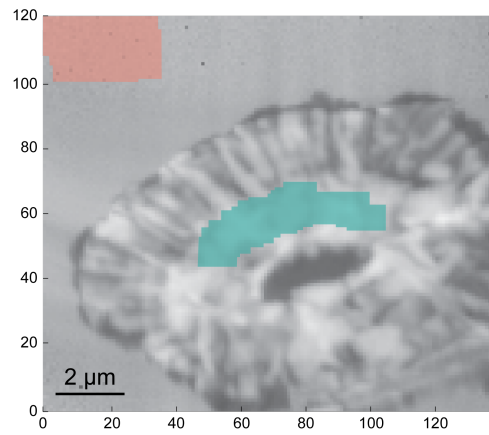
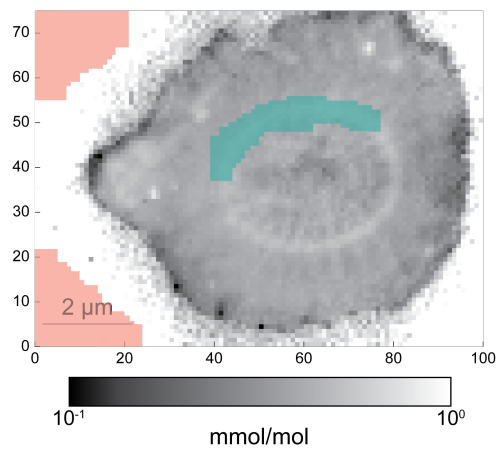


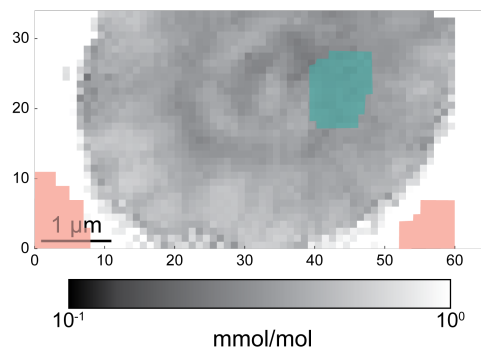
Figure S1. Ca (blue), Sr (red) and Mn (green) maps (free scale cps) of *C. crassus*, *W. contracta* and *D. striatus*.



Crepidolithus crassus



Watznaueria contracta



Discorhabdus striatus

Figure S2. Selected zone (green) and background (red) used for calculations in [Table 1](#) over Sr/Ca (mmol/mol) maps for *C. crassus*, *W. contracta* and *D. striatus*.